

# On the interaction of a moving hollow vortex with an aerofoil, with application to sound generation

By F. G. LEPPINGTON<sup>1</sup> AND R. A. SISSON<sup>2</sup>

<sup>1</sup>Department of Mathematics, Imperial College, London SW7 2BZ, UK

<sup>2</sup>Surpac Software International, PO Box 233, Belmont, Western Australia 6104

(Received 8 August 1995 and in revised form 16 April 1997)

A hollow vortex in the form of a straight tube, parallel to the  $z$ -axis, and of radius  $a$ , moves in a uniform stream of fluid with velocity  $U$  in the  $x$ -direction, with  $U$  small compared with the sound speed  $c$ . This steady flow is disturbed by the presence of a thin symmetric fixed aerofoil. With a change of  $x$ -coordinate, the problem is equivalent to that of a moving aerofoil cutting through an initially fixed vortex in still fluid. The aim of this work is to determine the resulting perturbed flow, and to estimate the distant sound field. A detailed calculation is given for the perturbed velocity potential in the incompressible flow case, for the linearized equations in the limit of small aerofoil thickness. A formally exact solution involves a four-fold integral and an infinite sum over all mode numbers. For the important special case where the vortex tube has small radius  $a$  compared with the aerofoil width, the deformed vortex is characterized by a hypothetical vortex filament located at the ‘mean centre’  $\bar{x}(z, t), \bar{y}(z, t)$  of the tube. Explicit results are given for  $\bar{x}(z, t), \bar{y}(z, t)$  for the case where the aerofoil has the elementary rectangular profile; results can then be obtained for more general and realistic cylindrical aerofoils by a single integral weighted with the derivative of the aerofoil thickness function. Finally the distant sound field is estimated, representing the aerofoil by a distribution of moving monopole sources and representing the effect of the deformed vortex in terms of compressible dipoles along the mean centre of the vortex.

---

## 1. Introduction

Many problems in hydro- and aero-dynamics involve the interaction between surfaces and regions of vorticity. Cavitated vortex tubes shed from the tip of an underwater propeller will interact with the local flow and with the moving vessel. Another important application, which is borne mainly in mind in this work, is that of the external noise from helicopters, arising from an interaction of vortex tubes and rotors. The flow around lifting (aerofoil) surfaces generates vortex sheets, shed by the action of viscosity at the trailing edges. These unstable sheets roll up to form thin vortex tubes: see, for example, Moore (1974), Moore & Saffman (1973). The fluid velocity is relatively large near a vortex core, so interactions with following rotors lead to unsteady flows and can induce significant sound fields.

There are several mechanisms which can contribute to the generation of sound in this context, and many authors have studied various aspects of the problem. The review articles by Janakiram (1990) and Schmitz & Yu (1986) discuss several general

aspects and provide many useful references. The fundamental papers of Lighthill (1952), Curle (1955) and Ffowcs Williams & Hawkings (1969) provide generally valid identities for sound fields in terms of local flow variables such as the force distribution on fixed or moving bodies in the flow field. The influence of vorticity has been described explicitly by Howe (1975), Mohring (1978) and Powell (1964, 1995) for example. Ffowcs Williams & O'Shea (1970) analysed the sound field due to a hollow vortex that is disturbed by an oscillatory point source; Sozou (1990) has considered the resonant interaction of a plane sound wave with a Rankine vortex.

There are several papers that deal specifically with problems on the interaction of moving vortices with aerofoils. Howe (1991) provides estimates for the generation of sound in fluid-structure problems with particular reference to a vortex interacting with a shrouded rotor in a duct. Hawkings (1978) has proposed a mechanism for the radiation of sound due to the unsteady drag on an aerofoil. The method of matched asymptotic expansions was used by Kambe (1986) to analyse the sound generated by vortex motion in the presence of solid or sharp bodies. The problem of sound produced by gusts passing an aerofoil has been addressed by Amiet (1986*a*) and this approach has been extended considerably by the same author and collaborators in later works. The effects of axial flow down the vortex core are important; the generation of sound from a steady axial flow, cut by a supersonically moving aerofoil, has been analysed by Ffowcs Williams & Guo (1988).

The present work concerns an idealization of the basic problem of a vortex that convects past a single aerofoil  $\mathcal{A}$ . A straight or nearly straight vortex has quite different characteristics according to whether it is nearly parallel with, or perpendicular to, the axis of the aerofoil. This paper is confined to the latter possibility, which is most relevant to the interaction of a vortex that is shed from the main rotor before being cut by one of the tail rotors.

The elementary line vortex model is useful in some contexts although it is unrealistic in having unbounded velocity (therefore unbounded negative pressure) near its axis. The model is not appropriate for our task of dealing with deformations of a vortex when it crosses an aerofoil, and a finite core radius is essential. The azimuthal velocity profile inside a real vortex core is complicated. In the most elementary model, to be investigated in detail here, the interior is replaced by a cylindrical cavity of negligible density and its surface is represented by a condition of constant pressure. This corresponds to the interior vapour pressure in the underwater case. This 'hollow vortex' model is perhaps less realistic in the aerodynamical context, but it has the advantage of being amenable to analytical treatment and is taken as a first step.

Suppose that such a hollow vortex tube, given in Cartesian coordinates by  $x^2 + y^2 < a^2$ ,  $-\infty < z < \infty$ , and with given exterior circulation  $K$ , is cut by a thin symmetric aerofoil that moves in the negative  $x$ -direction with speed  $U$ , small compared with the sound speed  $c$ , and cuts through the vortex. In the absence of the aerofoil, there is an irrotational circulatory flow for  $x^2 + y^2 > a^2$ , with zero velocity for  $x^2 + y^2 < a^2$ ; the discontinuity in tangential velocity at the surface implies a cylindrical vortex sheet there. Viewed from a reference frame  $(x_1, y_1, z_1)$  fixed in the aerofoil, the problem is that of a fixed aerofoil with a vortex that moves in the positive  $x_1$ -direction. It is conceptually easiest to imagine the aerofoil to be cusped at its leading edge, so the vortex is cut cleanly: for a rounded leading edge, the deformed vortex would pass from the upper to lower surface via the leading edge, and it is argued that viscous action would remove the thin part of the vortex joining the upper and lower surfaces.

For this first model, the aerofoil is at zero angle of incidence, with no circulation around it. This ensures that the flow is symmetric about the plane  $z = 0$ ; it is

therefore sufficient to confine attention to the half-space  $z > 0$ , with a vortex passing over a plane ( $z = 0$ ) with a hump that corresponds to the upper half of the aerofoil. The model allows for the distortion of the vortex as it passes the aerofoil. It does not include the separate effect, at a lifting aerofoil, whereby the vortex tube on the upper and lower surfaces would reach the trailing edge at different times, and at different places in general, because the spanwise flow is likely to be different on upper and lower surfaces. That mechanism is potentially very important but needs a separate analysis.

Amiet (1986*b*, 1990) has considered the case of an aerofoil that intersects a vortex at an angle different from  $90^\circ$ , using linearized aerofoil theory to derive a pressure fluctuation that is proportional to the vortex strength. The problem under discussion in the present paper is similar to that considered by Howe (1989). That analysis allows for different internal structures in the vortex, and takes account of its distortion as it passes the aerofoil. A formula for the surface forces is used to predict a sound field of dipole type with strength proportional to the square of the circulation  $K$  and this is contrasted with earlier results by Hawkings (1978) that have linear dependence on the circulation.

The present work deals with the hollow vortex, with a view to finding the local flow field and, in particular, the distortion of the free surface of the vortex as it passes the aerofoil. Detailed consideration is given first to the case of incompressible fluid, with a view to later extension to allow for the effects of compressibility. The governing equations are given in §2, and are linearized with respect to the small aerofoil thickness parameter  $\epsilon$ . A formally exact solution is derived in §3, in terms of a four-fold integral and an infinite sum over modes, for the velocity potential and for the perturbed position of the vortex surface from its mean position. When the vortex has small radius  $a$ , it can be represented in terms of a thin filament located at the ‘mean centre’  $\bar{x}(z, t), \bar{y}(z, t)$  of the actual tube. Explicit expressions are given in §4 for  $\bar{x}(z, t)$  and  $\bar{y}(z, t)$ , for the particular case of a two-dimensional aerofoil with rectangular cross-section. Corresponding results for any cross-section  $h(x_1)$  are then given in terms of integrals weighted with the derivative of the shape function  $h(x_1)$ . The effects of compressibility are incorporated in §5, representing the aerofoil by a distribution of moving monopole sources and representing the vortex distortion by a distribution of dipole sources along the  $z$ -axis with moments proportional to  $(-\bar{y}(z, t), \bar{x}(z, t))$  at height  $z$  and time  $t$ . The results are interpreted with reference to those for the related problem considered by Howe (1989). Numerical results are presented for a particular case.

## 2. Governing equations: incompressible flow problem

A hollow vortex in the form of a circular cylinder of radius  $a$ , with its axis parallel to the  $z$ -axis, moves in a uniform stream  $U$  of incompressible fluid, in the  $x_1$ -direction, past a thin aerofoil that is symmetric about its mid-plane  $z_1 = 0$ .

In the absence of the aerofoil, the velocity field outside the vortex has only a transverse component  $v_\theta = K/(2\pi r)$ , where  $K$  is the circulation and  $(r, \theta)$  denote polar coordinates based at the centre of the vortex. This steady circulatory flow is disturbed by the presence of an aerofoil whose surface is given by

$$z_1 = \pm \epsilon h(x_1, y_1), \quad (x_1, y_1) \in \mathcal{A}', \quad (2.1)$$

with  $h = 0$  outside some domain  $\mathcal{A}'$  which represents its planform. The parameter  $\epsilon$  is small compared with the minimum diameter of  $\mathcal{A}'$ .

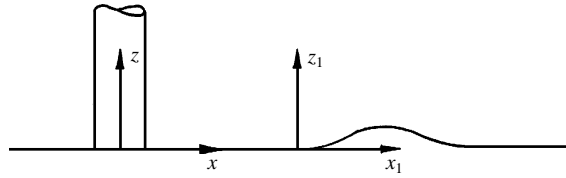


FIGURE 1. The vortex is given by  $x^2 + y^2 < a^2, z > 0$ ; the aerofoil is between  $x_1 = 0$  and  $x_1 = L$ .

It is convenient to use a reference frame  $(x, y, z)$  that is fixed relative to the vortex, thus

$$x = x_1 - Ut, \quad y = y_1, \quad z = z_1, \quad (2.2)$$

and to define the constant

$$\kappa = K/2\pi, \quad (2.3)$$

so as to simplify the subsequent algebra. The velocity potential is denoted by  $\phi(x, y, z; t)$ .

The geometry of the problem is indicated in figure 1. The even symmetry of the problem means that we need consider only the half-space  $z > 0$  and the undisturbed vortex has its surface at  $z \geq 0, r = a, -\pi \leq \theta \leq \pi$ , where  $(r, \theta, z)$  are cylindrical polars with  $r^2 = x^2 + y^2$ , and the upper surface of the aerofoil is given by

$$z = \epsilon h(x + Ut, y), \quad (x, y) \in \mathcal{A}, \quad (2.4)$$

where the (moving) planform  $\mathcal{A}$  corresponds to the domain  $\mathcal{A}'$ , expressed in term of  $(x, y)$ .

For a hollow vortex in incompressible fluid, and with no boundaries, the velocity field  $\mathbf{v} = (\kappa/r)\mathbf{e}_\theta$ , where  $\mathbf{e}_\theta$  is the unit vector in the  $\theta$ -direction, has potential  $\phi_0$  given by

$$\phi_0 = \kappa\theta. \quad (2.5)$$

Suppose now that this steady flow is perturbed by the presence of the moving aerofoil  $\mathcal{A}$ . Let the total velocity potential be denoted by

$$\phi = \phi_0 + \epsilon\psi(r, \theta, z; t). \quad (2.6)$$

The incompressibility requires that  $\psi$  be harmonic, thus

$$\nabla^2\psi = 0 \quad (2.7)$$

in the fluid region outside the vortex and above the plane  $z = 0$  and aerofoil  $\mathcal{A}$ . Boundary conditions are now required at the surface of the vortex and on the boundary  $z = 0$ .

### 2.1. Boundary condition at the vortex surface

There are two conditions to be applied at the surface of the vortex and, for the small disturbances envisaged here, these lead to conditions at its mean position ( $r = a$ ). The conditions are: (i) a kinematic requirement that particles at the interface remain there; and (ii) continuity of pressure, so that  $p = p_1$  at the interface. Suppose that the vortex surface is displaced slightly from its mean position at  $r = a$ , thus

$$r = a + \epsilon g(\theta, z; t). \quad (2.8)$$

The kinematic condition can be expressed as

$$\frac{D}{Dt}(r - a - \epsilon g) = 0, \quad (2.9)$$

where  $D/Dt$  is the total derivative  $\partial/\partial t + \mathbf{v} \cdot \nabla = \partial/\partial t + \nabla\phi \cdot \nabla$ . Substitution of the potential (2.6) and linearization for small values of  $\epsilon$  leads to the condition

$$\frac{\partial\psi}{\partial r} = \frac{\partial g}{\partial t} + \frac{\kappa}{a^2} \frac{\partial g}{\partial \theta} \quad \text{on } r = a. \quad (2.10)$$

Continuity of pressure requires  $p = p_1$  on the vortex interface. Bernoulli's equation gives

$$\frac{p}{\rho_0} + \frac{\partial\phi}{\partial t} + \frac{1}{2}(\nabla\phi)^2 = F(t), \quad (2.11)$$

where  $F(t)$  depends on time but not on position. The requirement  $p = p_1$  at  $r = a + \epsilon g$  leads to the linearized condition

$$\frac{\partial\psi}{\partial t} + \frac{\kappa}{a^2} \frac{\partial\psi}{\partial \theta} = \frac{\kappa^2}{a^3} g. \quad (2.12)$$

The conditions (2.10) and (2.12) can be combined to eliminate the (unknown) function  $g$  that specifies the distortion of the vortex surface, to get

$$\frac{\partial\psi}{\partial r} = \mathcal{L}\psi \quad (2.13)$$

at the mean surface  $r = a$ , where the operator  $\mathcal{L}$  is defined as

$$\mathcal{L} = \frac{a^3}{\kappa^2} \left( \frac{\partial}{\partial t} + \frac{\kappa}{a^2} \frac{\partial}{\partial \theta} \right)^2. \quad (2.14)$$

### 2.2. Boundary condition at the bottom surface

The bottom boundary consists of the moving surface  $z = \epsilon h$ , given by (2.4) for  $(x, y) \in \mathcal{A}$  and the plane region  $z = 0$  for  $(x, y) \notin \mathcal{A}$ . Both can be accommodated by the condition

$$z = \epsilon h(r \cos \theta + Ut, r \sin \theta), \quad (2.15)$$

with the understanding that  $h = 0$  when  $(x, y) \notin \mathcal{A}$ , and with  $x = r \cos \theta$ ,  $y = r \sin \theta$ . As the bottom is impermeable, particles on that surface always remain there, hence

$$\frac{D}{Dt}(z - \epsilon h) = 0 \quad (2.16)$$

on  $z = \epsilon h$ , where  $D/Dt$  is the total derivative  $\partial/\partial t + \mathbf{v} \cdot \nabla$ . For small values of  $\epsilon$ , this equation can be linearized to get

$$\frac{\partial\psi}{\partial z} = f \quad (2.17)$$

at  $z = 0$ , where  $f$  is given in terms of the thickness function  $h$  by

$$f(x, y; t) = \left( \frac{\partial}{\partial t} + \frac{\kappa}{r^2} \frac{\partial}{\partial \theta} \right) h(r \cos \theta + Ut, r \sin \theta). \quad (2.18)$$

### 2.3. Problem for $\psi$

The function  $\psi$  is harmonic in the region  $r > a, z > 0$ , and is subject to the boundary condition (2.13) at  $r = a$  and condition (2.17) at  $z = 0$ . Thus

$$\nabla^2\psi = 0, \quad r > a, z > 0, \quad (2.19)$$

$$\frac{\partial \psi}{\partial r} = \mathcal{L}\psi, \quad r = a, z > 0, \quad (2.20)$$

$$\frac{\partial \psi}{\partial z} = f, \quad r > a, z = 0, \quad (2.21)$$

where  $\mathcal{L}$  is the operator defined by (2.14), and the forcing function  $f$  is given by (2.18). Finally there is the condition that  $\psi \rightarrow 0$  as  $x^2 + y^2 + z^2 \rightarrow \infty$ .

### 3. Formulation and Green's function

The problem summarized by equations (2.19)–(2.21) can be solved exactly, in principle, to get a representation for  $\psi$  in terms of a Green function weighted with the forcing function  $f$  that appears in the boundary condition (2.21). Let  $\mathcal{G}(r, r', \theta, z; t)$  denote the Green function defined, for  $r > a, r' > a$ , by the equations

$$\nabla^2 \mathcal{G} = \frac{2}{r'} \delta(r - r') \delta(\theta) \delta(z) \delta(t), \quad r > a, r' > a, \quad (3.1)$$

$$\frac{\partial \mathcal{G}}{\partial r} = \mathcal{L}\mathcal{G} \quad \text{at} \quad r = a, \quad (3.2)$$

where  $\mathcal{L}$  is the differential operator given by formula (2.14). The function  $\mathcal{G}$  is even in  $z$  and represents the potential at  $\mathbf{r} = (r, \theta, z)$  due to a source of strength  $2\delta(t)$  at  $(r, \theta, z) = (r', 0, 0)$ . It follows that the normal velocity on the plane  $z = 0$  is given by

$$\frac{\partial \mathcal{G}}{\partial z} = \pm \frac{1}{r'} \delta(r - r') \delta(\theta) \delta(t) \quad \text{at} \quad z = \pm 0. \quad (3.3)$$

Let

$$\mathcal{G} = \mathcal{G}_1 + \mathcal{G}_2, \quad (3.4)$$

where

$$\mathcal{G}_1 = -\delta(t)/(2\pi R), \quad \text{with} \quad R = (r^2 + r'^2 - 2rr' \cos \theta + z^2)^{1/2}, \quad (3.5)$$

satisfies the equations (3.1) and (3.3).

Thus  $\mathcal{G}_2$  is harmonic for  $r > a$  and is subject to the boundary condition

$$\frac{\partial \mathcal{G}_2}{\partial r} - \mathcal{L}\mathcal{G}_2 = -\frac{\partial \mathcal{G}_1}{\partial r} + \mathcal{L}\mathcal{G}_1, \quad r = a, \quad (3.6)$$

where the right-hand side is a known function of  $\theta, z$  and  $t$ , with  $\mathcal{G}_1$  given by (3.5). The geometry of the problem suggests a solution using a Fourier series with respect to  $\theta$  and Fourier integration with respect to  $z$ . Thus we define

$$\overline{\mathcal{G}}_n(r, r'; s; t) = \frac{1}{2\pi} \int_{-\infty}^{\infty} \int_{-\pi}^{\pi} \mathcal{G}(r, r', \theta, z; t) e^{isz} e^{-in\theta} d\theta dz, \quad (3.7)$$

with inversion formula

$$\mathcal{G}(r, r', \theta, z; t) = \frac{1}{2\pi} \sum_{n=-\infty}^{\infty} e^{in\theta} \int_{-\infty}^{\infty} \overline{\mathcal{G}}_n(r, r'; s; t) e^{-isz} ds. \quad (3.8)$$

The transform pair may be applied with  $\mathcal{G}$  given in turn by  $\mathcal{G}_1$  and  $\mathcal{G}_2$ , with respective transforms  $\overline{\mathcal{G}}_{1n}(r, r'; s; t)$  and  $\overline{\mathcal{G}}_{2n}(r, r'; s; t)$ .

3.1. Fourier series-integral representation for  $\mathcal{G}_1$

As  $\mathcal{G}_1$  is an even function of  $z$ , the transform  $\overline{\mathcal{G}}_{1n}$  is also even in  $s$ . Both functions have the simple multiplicative time dependence  $\delta(t)$ , where  $\delta$  denotes the Dirac delta function. Note that  $\mathcal{G}_1$  satisfies equation (3.1); multiplication by  $\exp(isz - in\theta)$  and integration with respect to  $z$  and  $\theta$  leads to the corresponding equation for  $\overline{\mathcal{G}}_{1n}$ , namely

$$r^2 \frac{\partial^2 \overline{\mathcal{G}}_{1n}}{\partial r^2} + r \frac{\partial \overline{\mathcal{G}}_{1n}}{\partial r} - (s^2 r^2 + n^2) \overline{\mathcal{G}}_{1n} = \frac{r'}{\pi} \delta(r - r') \delta(t). \quad (3.9)$$

Solutions of the homogeneous version of this equation are the modified Bessel functions  $I_n(|s|r)$  and  $K_n(|s|r)$ ;  $I_n(\eta)$  is finite as  $\eta \rightarrow 0$  but infinite as  $\eta \rightarrow \infty$ , whilst  $K_n(\eta)$  is singular at  $\eta = 0$  and is exponentially small as  $\eta \rightarrow \infty$ . Thus we take

$$\overline{\mathcal{G}}_{1n} = A_n I_n(|s|r_<) K_n(|s|r_>) \delta(t), \quad (3.10)$$

where  $r_<$  and  $r_>$  denote the lesser and greater of  $r$  and  $r'$ . The formula (3.10) ensures that  $\overline{\mathcal{G}}_{1n}$  is continuous at  $r = r'$ , and  $A_n$  is determined from (3.9) which requires the discontinuity condition

$$[\partial \overline{\mathcal{G}}_{1n} / \partial r]_{r'-0}^{r'+0} = (\pi r')^{-1} \delta(t). \quad (3.11)$$

Thus  $A_n = -(1/\pi)$ , where use has been made of the Wronskian relation

$$I_n(\eta) K_n'(\eta) - I_n'(\eta) K_n(\eta) = -1/\eta, \quad (3.12)$$

and

$$\mathcal{G}_1 = -\frac{\delta(t)}{2\pi^2} \sum_{-\infty}^{\infty} \int_{-\infty}^{\infty} I_n(|s|r_<) K_n(|s|r_>) \exp(in\theta - isz) ds \quad (3.13)$$

is the Fourier series-integral form for the elementary Green function  $\mathcal{G}_1$  given by formula (3.5). The point of this representation is that the harmonic function  $\mathcal{G}_2$  can now be expressed in a similar form that allows us to apply the boundary condition (3.6).

3.2. Fourier series-integral representation for  $\mathcal{G}_2$

Let  $\overline{\mathcal{G}}_{2n}$  be the transform of  $\mathcal{G}_2$ , where this pair of functions is related by formulae (3.7) and (3.8). The governing equation for  $\overline{\mathcal{G}}_{2n}$  is the homogeneous version of (3.9), namely

$$r^2 \frac{\partial^2 \overline{\mathcal{G}}_{2n}}{\partial r^2} + r \frac{\partial \overline{\mathcal{G}}_{2n}}{\partial r} - (s^2 r^2 + n^2) \overline{\mathcal{G}}_{2n} = 0 \quad \text{for } r > a, -\infty < z < \infty, \quad (3.14)$$

and it remains to satisfy the boundary condition (3.6) which has the transformed equivalent

$$\frac{\partial \overline{\mathcal{G}}_{2n}}{\partial r} - \overline{\mathcal{L}} \overline{\mathcal{G}}_{2n} = -\frac{\partial \overline{\mathcal{G}}_{1n}}{\partial r} + \overline{\mathcal{L}} \overline{\mathcal{G}}_{1n} \quad \text{at } r = a, \quad (3.15)$$

with

$$\overline{\mathcal{L}} = \frac{a^3}{\kappa^2} \left( \frac{\partial}{\partial t} + \frac{in\kappa}{a^2} \right)^2. \quad (3.16)$$

In order to ensure boundedness as  $r \rightarrow \infty$ , the  $I_n$  solutions of (3.14) are excluded, hence

$$\overline{\mathcal{G}}_{2n} = (C_n/\pi) K_n(|s|r). \quad (3.17)$$

The coefficient  $C_n$  has to be chosen so that  $\overline{\mathcal{G}}_{2n}$  satisfies a causality condition as

well as the boundary condition (3.15) on the cylinder  $r = a$ . It is found convenient to express  $C_n$  in the form

$$C_n = \frac{I_n(|s|a)K_n(|s|r')\delta(t)}{K_n(|s|a)} - P_n(t), \quad (3.18)$$

whence substitution into the boundary condition (3.15) gives

$$\left\{ \left( \frac{\partial}{\partial t} + \frac{i n \kappa}{a^2} \right)^2 - \frac{\kappa^2 |s| K_n'(|s|a)}{a^3 K_n(|s|a)} \right\} P_n = \frac{\kappa^2 K_n(|s|r')}{a^4 K_n^2(|s|a)} \delta(t). \quad (3.19)$$

The solutions of the homogeneous version of this equation are  $\exp(\lambda_1 t)$  and  $\exp(\lambda_2 t)$ , where

$$\lambda_1 = (-i\kappa n + i\kappa\mu_n)/a^2, \quad \lambda_2 = (-i\kappa n - i\kappa\mu_n)/a^2, \quad (3.20)$$

with

$$\mu_n = \{-|s|aK_n'(|s|a)/K_n(|s|a)\}^{1/2}. \quad (3.21)$$

The solution which is causal (that is,  $P_n = 0$  for  $t < 0$ ) and which satisfies the discontinuity requirement

$$[dP_n/dt] = (\kappa^2/a^4)K_n(|s|r')/\{K_n(|s|a)\}^2, \quad (3.22)$$

that follows from equation (3.19), is found to be

$$P_n(t) = -\frac{i\kappa}{2a^2\mu_n} \frac{K_n(|s|r')}{K_n(|s|a)^2} (e^{\lambda_1 t} - e^{\lambda_2 t})H(t), \quad (3.23)$$

where  $H(t)$  is the Heaviside step function. Thus, on writing  $\mathcal{G}_2$  as a sum of terms  $\mathcal{G}_{21} + \mathcal{G}_{22}$ , which are respectively proportional to  $\delta(t)$  and  $H(t)$  and which originate from the respective terms on the right-hand side of (3.18), we have

$$\mathcal{G} = \mathcal{G}_1 + \mathcal{G}_{21} + \mathcal{G}_{22} \quad \text{for } r > a, r' > a, \quad (3.24)$$

where

$$\mathcal{G}_1 = -\frac{\delta(t)}{2\pi R} = -\frac{\delta(t)}{2\pi^2} \sum_{-\infty}^{\infty} \int_{-\infty}^{\infty} I_n(|s|r_<)K_n(|s|r_>) \exp(in\theta - isz) ds, \quad (3.25)$$

$$\mathcal{G}_{21} = \frac{\delta(t)}{2\pi^2} \sum_{-\infty}^{\infty} \int_{-\infty}^{\infty} \frac{I_n(|s|a)K_n(|s|r')}{K_n(|s|a)} K_n(|s|r) \exp(in\theta - isz) ds, \quad (3.26)$$

$$\begin{aligned} \mathcal{G}_{22} &= -\frac{1}{2\pi^2} \sum_{-\infty}^{\infty} \int_{-\infty}^{\infty} P_n(t) K_n(|s|r) \exp(in\theta - isz) ds \\ &= -\frac{H(t)\kappa}{2\pi^2 a^2} \sum_{-\infty}^{\infty} \int_{-\infty}^{\infty} \frac{\sin(\kappa\mu_n t/a^2)}{\mu_n} \frac{K_n(|s|r')K_n(|s|r)}{(K_n(|s|a))^2} \exp(in\theta - isz - i\kappa n t/a^2) ds. \end{aligned} \quad (3.27)$$

Note that  $\mathcal{G}_1 + \mathcal{G}_{21}$  is proportional to the delta function  $\delta(t)$ . The sum of terms is non-zero only at  $t = 0$ , has the appropriate source singularity at  $(r, \theta, z) = (r', 0, 0)$  and satisfies the 'acoustically soft' boundary condition

$$\mathcal{G}_1 + \mathcal{G}_{21} = 0 \quad (3.28)$$

at the vortex surface. It is the function  $\mathcal{G}_{22}$  that accounts for the waviness of the perturbed hollow vortex.



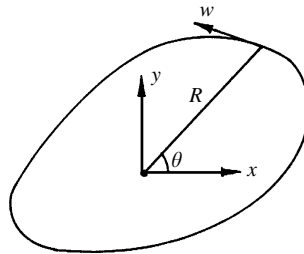


FIGURE 2. The cross-section of the disturbed vortex is given by  $r = R(\theta, z, t)$ ; the tangential velocity is  $w$ .

### 3.3. Solution for $\psi(r, \theta, z; t)$

The perturbation potential  $\psi(r, \theta, z; t)$  is given in terms of the Green function  $\mathcal{G}$  by the formula

$$\psi(r, \theta, z; t) = \int_{-\infty}^{\infty} dt' \iint_S f(x', y', t') \mathcal{G}(r, r', \theta - \theta', z; t - t') dx' dy', \quad (3.29)$$

where  $S$  is the region  $x'^2 + y'^2 > a^2$  and  $f$  is the function (2.18).

## 4. Effective line vortex

The expression (3.29) gives a formally exact solution for the potential  $\psi$ , and hence for the distortion  $\epsilon g(\theta, z, t)$  of the surface of the vortex, according to formulae (2.8) and (2.12). However, the calculation involves a four-fold integration (with respect to  $x', y', t'$  and the transform variable  $s$ ) and an infinite sum over all mode numbers  $n$ .

A further simplification is now made, based on the case where the vortex tube is thin: that is, the mean radius  $a$  is small compared with the aerofoil width  $L$ . In this case one can, for some purposes, usefully replace the hollow vortex by a hypothetical vortex filament placed at the ‘centre’ of the vortex tube, with details given below.

This approach has the advantage of reducing considerably the multiple integrals that are inherent in the full solution. It also has the important advantage of allowing the incorporation of compressibility effects, and estimates for the distant sound field. For according to Howe (1975), Powell (1995) and Leppington (1995), a moving line vortex in compressible fluid is acoustically equivalent to a moving line dipole or dipole sheet, directed along the common perpendicular to the mean flow and the line vortex. Such an estimate for the sound field is given in §5, and attention is now turned to the task of identifying the position of the equivalent vortex filament in the incompressible flow problem considered hitherto.

Consider the cross-section of the hollow vortex, at height  $z$  and time  $t$ , given by the closed curve

$$r = R(\theta) \equiv a + \epsilon g(\theta, z; t), \quad (4.1)$$

as shown in figure 2: the diagram is schematic as formula (4.1), with  $\epsilon$  small, implies that the contour is actually a small deformation from the circle of radius  $a$ .

Note that  $R$  depends also on  $z$  and  $t$ , but the latter will be omitted henceforth, for the sake of algebraic simplicity. There is no flow inside the vortex so the strength  $w$  of the vortex sheet, that occupies the deformed surface  $r = R(\theta)$ , is the tangential velocity there, namely  $w = \partial\phi/\partial s$ , where  $s$  is arclength. Thus the  $x$ -component of the

effective centre is given by

$$K\bar{x} = \int w x ds = \int_{-\pi}^{\pi} w(\theta) \cos \theta R^2 \left\{ 1 + \frac{1}{R^2} \left( \frac{dR}{d\theta} \right)^2 \right\}^{1/2} d\theta, \quad (4.2)$$

where

$$K = \int w ds = 2\pi\kappa$$

is the circulation and  $R$  is the function defined by formula (4.1). For small values of the parameter  $\epsilon$ , we pose the expansion

$$w = w_0 + \epsilon w_1 + \dots \quad (4.3)$$

to get

$$\bar{x} = \frac{\epsilon}{2\pi\kappa} \int_{-\pi}^{\pi} (a^2 w_1 + 2aw_0 g) \cos \theta d\theta. \quad (4.4)$$

Now the tangential velocity  $w$  is given by  $\partial\phi/\partial s$  where  $\phi = \phi_0 + \epsilon\psi$  is the total velocity potential, whence it is found that

$$w_0 = \frac{\kappa}{a}, \quad w_1 = \frac{1}{a} \frac{\partial\psi}{\partial\theta} - \frac{\kappa g}{a^2}, \quad (4.5)$$

with  $g$  given in terms of  $\psi$  by formula (2.12). Thus

$$\bar{x} = \frac{\epsilon/a}{2\pi\Gamma} \int_{-\pi}^{\pi} \left\{ 2 \frac{\partial\psi}{\partial\theta} + \frac{1}{\Gamma} \frac{\partial\psi}{\partial t} \right\} \cos \theta d\theta, \quad (4.6)$$

in terms of the perturbation potential  $\psi$ , and with

$$\Gamma = \frac{\kappa}{a^2} = \frac{K}{2\pi a^2}. \quad (4.7)$$

Similarly the  $y$ -component of the effective centre, at height  $z$  and time  $t$ , is given by

$$\bar{y} = \frac{\epsilon/a}{2\pi\Gamma} \int_{-\pi}^{\pi} \left\{ 2 \frac{\partial\psi}{\partial\theta} + \frac{1}{\Gamma} \frac{\partial\psi}{\partial t} \right\} \sin \theta d\theta. \quad (4.8)$$

The integrand of (4.6) is evaluated on the mean radius  $r = a$ ; hence, from (3.29) and (3.8),

$$\psi = \frac{1}{2\pi} \int_{-\infty}^t dt' \iint_S f(x', y', t') dx' dy' \sum_{n=-\infty}^{\infty} \int_{-\infty}^{\infty} \bar{\mathcal{G}}_n(a, r'; s; t-t') e^{in\theta - isz} ds, \quad (4.9)$$

with

$$\bar{\mathcal{G}}_n(a, r'; s; t) = -\frac{\Gamma}{\pi} \frac{K_n(|s|r')}{K_n(|s|a)} \frac{\sin(\Gamma \mu_n t)}{\mu_n} \exp(-i\Gamma n t). \quad (4.10)$$

Note that the  $\cos \theta$  term in the integrand of (4.6) ensures that only the terms  $n = \pm 1$  of the sum in (4.9) contribute to the integral expression (4.6) for  $\bar{x}$ . Thus one finds that

$$\bar{x} = -\frac{\epsilon/a}{2\pi^2} \int_{-\infty}^t dt' \iint_S f(x', y', t') dx' dy' \int_{-\infty}^{\infty} e^{-isz} \frac{K_1(|s|r')}{K_1(|s|a)} \frac{1}{\mu} P(t-t'; s) ds, \quad (4.11)$$

where

$$\mu = \mu_1 = \left\{ 1 + |s|a \frac{K_0(|s|a)}{K_1(|s|a)} \right\}^{1/2} \quad (4.12)$$

and

$$P(t) = \sin(\Gamma \mu t) \sin(\Gamma t + \theta') + \mu \cos(\Gamma \mu t) \cos(\Gamma t + \theta'). \quad (4.13)$$

Now in the limit of small  $a$ , with  $(r', z')$  fixed, it is argued that the main contribution to the  $s$ -integration comes from the vicinity of  $s = 0$ . Thus we make the approximations

$$K_1(|s|a) \sim (|s|a)^{-1} \quad \text{and} \quad \mu \sim 1, \quad (4.14)$$

whence

$$\int_{-\infty}^{\infty} \exp(-isz) \frac{K_1(|s|r')}{K_1(|s|a)} \mu^{-1} P(t; s) ds \sim 2a \cos \theta' \int_0^{\infty} s \cos(sz) K_1(sr') ds. \quad (4.15)$$

The latter integral can be evaluated exactly, using the result (see Watson 1944) that  $\int_0^{\infty} \cos(sz) K_0(sr') ds = (\pi/2)(z^2 + r'^2)^{-1/2}$ , which can be differentiated with respect to  $r'$  to get

$$\int_0^{\infty} s \cos(sz) K_1(sr') ds = (\pi/2)r'(z^2 + r'^2)^{-3/2}. \quad (4.16)$$

It follows that

$$\bar{x} = -\frac{\epsilon}{2\pi} \int_{-\infty}^t dt' \iint_S \frac{x' f(x', y', t')}{(x'^2 + y'^2 + z^2)^{3/2}} dx' dy'. \quad (4.17)$$

A similar procedure gives an analogous expression for  $\bar{y}$ , namely

$$\bar{y} = -\frac{\epsilon}{2\pi} \int_{-\infty}^t dt' \iint_S \frac{y' f(x', y', t')}{(x'^2 + y'^2 + z^2)^{3/2}} dx' dy'. \quad (4.18)$$

#### 4.1. Evaluation of $\bar{x}(z, t)$

The pair of formulae (4.17) and (4.18) give relatively simple representations for the mean centre  $(\bar{x}(z, t), \bar{y}(z, t))$  of the equivalent line vortex, in terms of the function  $f(x, y, t)$  that is related to the aerofoil shape,  $h(x, y)$ , according to the expression (2.18). To make further progress it is necessary to choose a particular shape function  $h(x_1, y_1)$  and the simplest prototype case is that of the 'top-hat' profile

$$h(x_1, y_1) = H(x_1) - H(x_1 - L), \quad (4.19)$$

independent of  $y_1$ , where  $H(x_1)$  denotes the Heaviside step-function. Such a rectangular aerofoil profile is not realistic, but it has the distinct advantage that it leads to explicit formulae for  $\bar{x}$  and  $\bar{y}$ . Furthermore, this basic special case can be used to generate more general profiles, by superposition, and this point will be taken up at the end of this section. According to (2.18), the function  $f$ , that appears in the integrand (4.17), is given by

$$f(x', y', t') = \{ \delta(x' + Ut') - \delta(x' + Ut' - L) \} \left\{ U - \frac{\kappa y'}{x'^2 + y'^2} \right\}, \quad (4.20)$$

where  $\delta$  is the Dirac delta function. Thus

$$\bar{x} = -\frac{\epsilon}{2\pi} \int_{t-L/U}^t Q_x dt', \quad (4.21)$$

with

$$Q_x = \iint_S \delta(x' + Ut') \left\{ U - \frac{\kappa y'}{x'^2 + y'^2} \right\} \frac{x'}{(x'^2 + y'^2 + z^2)^{3/2}} dx' dy', \quad (4.22)$$

evaluated over the region  $S$  ( $x'^2 + y'^2 > a^2$ ) outside the circle of radius  $a$ , and this integration can be performed exactly. Note first that the term proportional to  $\Gamma a^2 y'$  gives zero contribution as it is an odd function of  $y'$ . The delta function  $\delta(x' + Ut')$  picks out the value of the integrand on the line  $x' = -Ut'$ . If  $U|t'| > a$ , it is clear that the integral  $Q_x$  is the same as if the integration region were taken over the whole  $(x', y')$ -space; if  $U|t'| < a$ , on the other hand, the restricted domain  $S$  has to be accounted for. Thus one finds that

$$Q_x = -2U^2 t' \int_{\xi}^{\infty} (U^2 t'^2 + y'^2 + z^2)^{-3/2} dy', \quad (4.23)$$

where

$$\xi = 0 \quad \text{if } U|t'| > a; \quad \xi = (a^2 - U^2 t'^2)^{1/2} \quad \text{if } U|t'| < a, \quad (4.24)$$

and the integral (4.23) can be evaluated to get

$$Q_x = -\frac{2U^2 t'}{U^2 t'^2 + z^2} \left\{ 1 - \frac{(a^2 - U^2 t'^2)^{1/2} H(a^2 - U^2 t'^2)}{(a^2 + z^2)^{1/2}} \right\}. \quad (4.25)$$

It remains to perform the integration (4.21) with respect to  $t'$ . It is convenient to express the results in terms of the new variables  $\tau$ ,  $\tau'$  and  $\zeta$ , which are defined as

$$\tau' = Ut'/a; \quad \tau = Ut/a; \quad \zeta = z/a. \quad (4.26)$$

It is found that the integral (4.21) reduces to the solution:

$$\bar{x} = (\epsilon/2\pi) \{ P_x(\zeta, \tau) - P_x(\zeta, \tau - L/a) \}, \quad (4.27)$$

with

$$P_x(\zeta, \tau) = P_e(\zeta, \tau) \quad \text{if } |\tau| > 1, \quad (4.28)$$

$$P_x(\zeta, \tau) = P_e(\zeta, \tau) + p_e(\zeta, \tau) \quad \text{if } |\tau| < 1, \quad (4.29)$$

where

$$P_e(\zeta, \tau) = \ln(\tau^2 + \zeta^2), \quad (4.30)$$

$$p_e(\zeta, \tau) = \ln \frac{\{(1 + \zeta^2)^{1/2} + (1 - \tau^2)^{1/2}\}^2}{\tau^2 + \zeta^2} - 2 \frac{(1 - \tau^2)^{1/2}}{(1 + \zeta^2)^{1/2}}. \quad (4.31)$$

Note that both  $P_e$  and  $p_e$  are even functions of  $\tau$  and that  $p_e(\zeta, 1) = 0$ . It is seen that  $\bar{x}$  is an odd function of  $\tau - L/(2a)$ , hence of  $t - L/(2U)$ . Evidently  $\bar{x}$  has different forms in the five time régimes: (i)  $\tau < -1$ ; (ii)  $-1 < \tau < 1$ ; (iii)  $1 < \tau < (L/a) - 1$ ; (iv)  $(L/a) - 1 < \tau < (L/a) + 1$ ; (v)  $\tau > (L/a) + 1$ . Régime (i) is that before the vortex tube reaches the leading edge of the aerofoil, régime (ii) corresponds to the vortex passing the leading edge, with similar interpretations for the other time intervals (iii), (iv) and (v). In each of the régimes (i), (iii) and (v), for example,  $\bar{x}$  has the form

$$\bar{x} = \frac{\epsilon}{2\pi} \ln \left\{ \frac{\tau^2 + \zeta^2}{(\tau - L/a)^2 + \zeta^2} \right\}. \quad (4.32)$$

4.2. Evaluation of  $\bar{y}(z, t)$ 

A similar procedure can be followed for the evaluation of  $\bar{y}$  (formula (4.18)) for the case of the top-hat profile (4.19). One finds that

$$\bar{y} = -\frac{\epsilon}{2\pi} \int_{t-L/U}^t Q_y dt', \quad (4.33)$$

where  $Q_y$  has form similar to that in (4.22), except that  $x'$  is replaced by  $y'$  in the numerator of the integrand. In this case, the term proportional to  $U$  gives zero contribution, due to the odd symmetry with respect to  $y'$ , and we find

$$Q_y = -\frac{K}{2\pi} \iint_S \frac{\delta(x' + Ut')y'^2}{(x'^2 + y'^2)(x'^2 + y'^2 + z^2)^{3/2}} dx' dy', \quad (4.34)$$

where  $S$  is again the region  $x'^2 + y'^2 > a^2$ . If  $U|t'| > a$ , the value of  $Q_y$  is the same as if the integral (4.34) were taken over all  $(x', y')$ -space, and is readily evaluated. If  $U|t'| < a$ , on the other hand, due care is needed to deal with the restricted domain  $S$ , thus

$$Q_y = -\frac{K}{\pi} \int_{\xi}^{\infty} \frac{y'^2 dy'}{(U^2 t'^2 + y'^2)(U^2 t'^2 + y'^2 + z^2)^{3/2}} \quad \text{if } U|t'| > a, \quad (4.35)$$

where  $\xi$  is the number defined in (4.24). The results are conveniently represented in terms of the variables  $\tau'$ ,  $\tau$  and  $\zeta = z/a$  of formula (4.26). It is found that

$$Q_y = -\frac{K}{\pi a^2} G(\zeta, \tau'), \quad (4.36)$$

where

$$G(\zeta, \tau') = G_1(\zeta, \tau') \quad \text{if } |\tau'| > 1, \quad (4.37)$$

$$G(\zeta, \tau') = G_1(\zeta, \tau') + g_1(\zeta, \tau') \quad \text{if } |\tau'| < 1, \quad (4.38)$$

with  $G_1(\zeta, \tau')$  and  $g_1(\zeta, \tau')$  defined by

$$\zeta^2 G_1(\zeta, \tau') = \left\{ 1 - \frac{|\tau'|}{\zeta} \tan^{-1} \frac{\zeta}{|\tau'|} \right\}, \quad (4.39)$$

$$\zeta^2 g_1(\zeta, \tau') = -\frac{(1 - \tau'^2)^{1/2}}{(1 + \zeta^2)^{1/2}} + \frac{|\tau'|}{\zeta} \tan^{-1} \left\{ \frac{\zeta (1 - \tau'^2)^{1/2}}{|\tau'| (1 + \zeta^2)^{1/2}} \right\}, \quad \text{for } |\tau'| < 1. \quad (4.40)$$

It remains to evaluate the time integral (4.33), with  $t' = a\tau'/U$ , and this can be done explicitly in terms of the functions  $P_o(\tau)$  and  $p_o(\tau)$ , which are respectively integrals of  $G_1$  and  $g_1$ , as follows:

$$\zeta^2 P_o(\zeta, \tau) = \zeta^2 \int_0^{\tau} G_1(\zeta, \tau') d\tau' \quad (4.41)$$

$$= \frac{\pi\zeta}{4} \operatorname{sgn}\tau + \frac{\tau}{2} - \frac{\zeta^2 + \tau^2}{2\zeta} \operatorname{sgn}\tau \tan^{-1} \frac{\zeta}{|\tau|}; \quad (4.42)$$

$$\zeta^2 p_o(\zeta, \tau) = \zeta^2 \int_0^{\tau} g_1(\zeta, \tau') d\tau' \quad (4.43)$$

$$= \frac{\zeta^2 \sin^{-1} \tau}{2(1 + \zeta^2)^{1/2}} - \frac{\tau(1 - \tau^2)^{1/2}}{2(1 + \zeta^2)^{1/2}} + \frac{\zeta^2 + \tau^2}{2\zeta} \tan^{-1} \frac{\zeta(1 - \tau^2)^{1/2}}{\tau(1 + \zeta^2)^{1/2}} - \frac{\pi\zeta}{4} \operatorname{sgn}\tau, \quad (4.44)$$

for  $|\tau| < 1$ . Note that  $P_o$  and  $p_o$  are odd functions of (scaled) time  $\tau$ , and that

$$p_o(\zeta, 1) = (\pi/4)\{(1 + \zeta^2)^{-1/2} - \zeta^{-1}\}. \quad (4.45)$$

Thus the time-integral (4.33) can be accomplished, leading to the result

$$\bar{y} = \frac{\epsilon K}{2\pi^2 a U} \{P_y(\zeta, \tau) - P_y(\zeta, \tau - L/a)\}, \quad (4.46)$$

where

$$P_y(\zeta, \tau) = P_o(\zeta, \tau) - p_o(\zeta, 1) \quad \text{if } \tau < -1, \quad (4.47)$$

$$P_y(\zeta, \tau) = P_o(\zeta, \tau) + p_o(\zeta, \tau) \quad \text{if } -1 < \tau < 1, \quad (4.48)$$

$$P_y(\zeta, \tau) = P_o(\zeta, \tau) + p_o(\zeta, 1) \quad \text{if } \tau > 1. \quad (4.49)$$

It is seen that  $\bar{y}$  is an even function of the (scaled) time variable  $\tau - L/(2a)$ , hence of the time  $t - L/(2U)$ . Expressions (4.27) and (4.46) provide explicit formulae for the location of the equivalent vortex filament at time  $t = a\tau/U$  and height  $z = a\zeta$ .

#### 4.3. Values near $\zeta = 0$ and near $\tau = 0$

The forms (4.28)–(4.31) and (4.41)–(4.44) appear to have singular behaviour as  $\zeta \rightarrow 0$  or  $\tau \rightarrow 0$ , but the singularities cancel between the various terms. For the purpose of numerical evaluations of integrals, such as are required for the expression (5.46), with  $I_x$  and  $I_y$  defined by (5.42) and (5.43), it is desirable to determine the limiting forms for  $\ddot{P}_x$  ( $= d^2P_x/d\tau^2$ ) and  $\ddot{P}_y$  ( $= d^2P_y/d\tau^2$ ) when either or both of the variables  $\zeta, \tau$  may be small. It is found that

$$\ddot{P}_x \sim 1, \quad \ddot{P}_y \sim -\tau/4 \quad \text{as } \tau \rightarrow 0, \quad \zeta \rightarrow 0; \quad (4.50)$$

$$\ddot{P}_x \sim \frac{2}{\zeta^2} \left\{ \frac{(1 + \zeta^2)^{1/2} - 1}{(1 + \zeta^2)^{1/2}} \right\}, \quad \ddot{P}_y \sim \frac{\tau}{\zeta^4} \left\{ \frac{2(1 + \zeta^2)^{1/2} - (2 + \zeta^2)}{(1 + \zeta^2)^{1/2}} \right\}, \quad (4.51)$$

as  $\tau \rightarrow 0$ , with  $\zeta$  fixed;

$$\ddot{P}_x \sim -\frac{2}{\tau^2}, \quad \ddot{P}_y \sim -\frac{2}{3\tau^3}, \quad \text{as } \zeta \rightarrow 0, \quad |\tau| > 1; \quad (4.52)$$

$$\ddot{P}_x \sim \frac{2}{\tau^2} \left\{ \frac{1 - (1 - \tau^2)^{1/2}}{(1 - \tau^2)^{1/2}} \right\}, \quad \ddot{P}_y \sim \left\{ \frac{-2 + (1 - \tau^2)^{1/2}(2 + \tau^2)}{3\tau^3} \right\}, \quad (4.53)$$

as  $\zeta \rightarrow 0$ , with  $|\tau| < 1$  and fixed.

Note that  $\ddot{P}_x$  has an integrable (inverse square root) singularity as  $\tau \rightarrow 1$ .

#### 4.4. General aerofoil cross-section

The results (4.27) and (4.46) have been derived for the special case of a two-dimensional aerofoil whose cross-section  $h(x_1)$  has the top-hat profile given by (4.19). A general cross-section  $h(x_1)$  (with  $h = 0$  for  $x_1 \leq 0$  and for  $x_1 \geq L$ ) can be generated by the identity

$$h(x_1) = - \int_0^L \frac{dh(l)}{dl} \{H(x_1) - H(x_1 - l)\} dl. \quad (4.54)$$

By linear superposition, the solution for  $\psi$ , and also  $(\bar{x}, \bar{y})$ , can be inferred. Thus

$$\bar{x} = \frac{\epsilon}{2\pi} \int_0^L \frac{dh(l)}{dl} P_x(\zeta, \tau - l/a) dl, \quad (4.55)$$

$$\bar{y} = \frac{\epsilon K}{2\pi^2 a U} \int_0^L \frac{dh(l)}{dl} P_y(\zeta, \tau - l/a) dl, \quad (4.56)$$

with  $P_x$  and  $P_y$  defined by (4.28), (4.29) and (4.47)–(4.49).

## 5. The sound field

The calculations described in §§2–4 are for the evolution of a thin hollow vortex in *incompressible* flow. The present section concerns the effects of compressibility. If the Mach number  $M$ , given by

$$M = U/c, \quad (5.1)$$

is small, where  $U$  is the flow speed and  $c$  is the mean sound speed, then the incompressible flow can be matched onto a sound field, valid at distances  $\gg a$  from the vortex.

The sound field can be attributed to two effects, arising from the imposed velocity (2.21) and from the the distortion  $(\bar{x}, \bar{y})$  of the effective line vortex. It is convenient to refer to these respective contributions as ‘displacement sound’ and ‘vortex sound’, but it is noted that the vortex deflection is itself a result of the aerofoil displacement. Thus we may express the compressible sound field  $\phi_c$  (the outer potential in the language of matched asymptotic expansions) as the sum of terms

$$\phi_c = \phi_{dis} + \phi_{vor}, \quad (5.2)$$

and these are calculated separately as follows.

### 5.1. Displacement sound

The potential  $\phi_{dis}$  is subject to the acoustic wave equation, together with the boundary condition (from (2.21))

$$\frac{\partial \phi_{dis}}{\partial z} = \pm \epsilon f(x, y; t) H(x^2 + y^2 - a^2) \quad \text{at } z = \pm 0, \quad (5.3)$$

where  $H$  denotes the Heaviside step-function and  $f$  is given in terms of the aerofoil thickness function  $h$  according to expression (2.18). Note that  $f \neq 0$  only on that part  $\mathcal{A}$  of the  $(x, y)$ -plane that corresponds to the (moving) planform of the aerofoil, and that  $\phi_{dis}$  is even with respect to  $z$ . The boundary condition (5.3) is equivalent to the presence of a source distribution of strength  $2\epsilon f(x, y; t) H(x^2 + y^2 - a^2)$ , per unit area, at the plane  $z = 0$ , in a compressible fluid. Thus  $\phi_{dis}$  is specified by the inhomogeneous wave equation

$$\left\{ \nabla^2 - \frac{1}{c^2} \frac{\partial^2}{\partial t^2} \right\} \phi_{dis} = 2\epsilon f(x, y; t) H(x^2 + y^2 - a^2) \delta(z). \quad (5.4)$$

For the particular case of the rectangular profile (4.19), the function  $f$  is proportional to the difference between a pair of delta functions and we have

$$\phi_{dis}(x, y, z; t) = \phi_{dis}^{(0)}(x, y, z; t) - \phi_{dis}^{(0)}(x, y, z; t - L/U), \quad (5.5)$$

where  $\phi_{dis}^{(0)}$  satisfies the equation

$$\left\{ \nabla^2 - \frac{1}{c^2} \frac{\partial^2}{\partial t^2} \right\} \phi_{dis}^{(0)} = 2\epsilon \left\{ U - \frac{K}{2\pi} \frac{y}{x^2 + y^2} \right\} \delta(x + Ut) \delta(z) H(x^2 + y^2 - a^2). \quad (5.6)$$

It is expedient to deal with the convective factor  $\delta(x + Ut)$  of equation (5.6) by means

of the Lorentz transformation

$$X = \beta(x + Ut), \quad Y = y, \quad Z = z, \quad T = \beta(t + Ux/c^2) \quad (5.7)$$

where  $c$  is the sound speed, and

$$\beta = (1 - M^2)^{-1/2}, \quad (5.8)$$

In particular,  $\beta \sim 1$  in the low Mach number limit envisaged here. In terms of the new variables,  $(X, Y, Z, T)$ , the equation (5.6) for  $\phi_{dis}^{(0)}$  reduces to the non-convective form

$$\left\{ \nabla_X^2 - \frac{1}{c^2} \frac{\partial^2}{\partial T^2} \right\} \phi_{dis}^{(0)} = \beta \delta(X) \delta(Z) q_0(Y, T), \quad (5.9)$$

where

$$q_0(Y, T) = q(Y, T) H(\beta^2 U^2 T^2 + Y^2 - a^2), \quad (5.10)$$

with

$$q(Y, T) = 2\epsilon \left\{ U - \frac{K}{2\pi} \frac{Y}{\beta^2 U^2 T^2 + Y^2} \right\}. \quad (5.11)$$

Evidently  $\phi_{dis}^{(0)}$  corresponds to a line distribution of sources, with explicit solution

$$\phi_{dis}^{(0)} = -\frac{\beta}{4\pi} \int_{-\infty}^{\infty} R^{-1} q_0(Y', T - R/c) dY', \quad (5.12)$$

with

$$R^2 = X^2 + Z^2 + (Y - Y')^2. \quad (5.13)$$

The corresponding contribution  $p_{dis}^{(0)}$  to the pressure is given by  $p_{dis}^{(0)} = -\rho_0 \partial \phi_{dis}^{(0)} / \partial t \equiv -\rho_0 \beta (\partial \phi_{dis}^{(0)} / \partial T + U \partial \phi_{dis}^{(0)} / \partial X)$ . In the far field, where  $R$  is large,

$$p_{dis}^{(0)} \sim \frac{\rho_0 \beta^2}{4\pi} \int_{-\infty}^{\infty} R^{-1} \left( 1 - M \frac{X}{R} \right) \frac{\partial q_0}{\partial T} dY'. \quad (5.14)$$

With a small value for the Mach number  $M$ ,  $\beta^2 \sim 1$  and  $MX/R \sim 0$ , hence

$$p_{dis}^{(0)} \sim \frac{\rho_0}{4\pi} \int_{-\infty}^{\infty} R^{-1} \frac{\partial q_0}{\partial T} (Y', T - R/c) dY', \quad (5.15)$$

with  $q_0$  given by (5.10). Thus the pressure field due to the displacement effect is given by

$$p_{dis} = p_{dis}^{(0)}(X, Y, Z; T) - p_{dis}^{(0)}(X - \beta L, Y, Z; T - \beta L/U), \quad (5.16)$$

with

$$p_{dis}^{(0)}(X, Y, Z; T) \sim I(X, Y, Z; T) + J(X, Y, Z; T), \quad (5.17)$$

where

$$I = \frac{\rho_0 U_1^2}{2\pi} \int_{-\infty}^{\infty} R^{-1} (T - R/c) q(Y', T - R/c) \delta(U_1^2 (T - R/c)^2 + Y'^2 - a^2) dY', \quad (5.18)$$

$$J = \frac{\rho_0}{4\pi} \int_{-\infty}^{\infty} R^{-1} \frac{\partial q}{\partial T} (Y', T - R/c) H(U_1^2 (T - R/c)^2 + Y'^2 - a^2) dY', \quad (5.19)$$

where

$$U_1 = \beta U \sim U. \quad (5.20)$$



The integral  $I$  has the form

$$I = \int_{-\infty}^{\infty} P(Y')\delta(g(Y'))dY' = \sum_i P(Y_i)/|g'(Y_i)|, \quad (5.21)$$

summed with respect to all the real values  $Y' = Y_i$  such that

$$g(Y') \equiv U_1^2(T - R/c)^2 + Y'^2 - a^2 = 0. \quad (5.22)$$

Clearly any real roots must be such that  $Y'^2 \leq a^2$ . Now  $R$  is large in the far field, so  $T$  must also be large for the existence of real roots of equation (5.22). Thus

$$R = R_0(1 - nY'/R_0 + \dots), \quad (5.23)$$

where

$$n = Y/R_0 \quad \text{and} \quad R_0^2 = X^2 + Y^2 + Z^2. \quad (5.24)$$

Defining the dimensionless variables  $\tau_1$  and  $\eta$  by the equations

$$a\tau_1 = U_1(T - R_0/c), \quad a\eta = Y', \quad (5.25)$$

where the suffix in  $\tau_1$  is used to distinguish this time-like variable from that used in §4, the function  $g$  has the approximate form

$$g \sim a^2\{(\tau_1 + M_2\eta)^2 + \eta^2 - 1\} \quad (5.26)$$

with

$$M_2 = \beta Mn \sim MY/R_0. \quad (5.27)$$

The roots of the quadratic expression (5.26), with  $M$  small, are

$$Y_1/a = \eta_1 = -\tau_1 M_2 - (1 + M_2^2 - \tau_1^2)^{1/2}, \quad Y_2/a = \eta_2 = -\tau_1 M_2 + (1 + M_2^2 - \tau_1^2)^{1/2}, \quad (5.28)$$

provided that  $\tau_1^2 \leq (1 + M_2^2)$ : there are no real roots for larger values of  $|\tau_1|$ . As  $M_2$  is small, the square-root factor can be approximated by  $(1 - \tau_1^2)^{1/2}$ . Thus the integral has the value

$$I \sim I^{(1)} + I^{(2)} \quad \text{for} \quad \tau_1^2 < 1, \quad (5.29)$$

where

$$I^{(1)} \sim \frac{\rho_0 U \epsilon}{2\pi R_0} (1 - \tau_1^2)^{-1/2} \{2U\tau_1\}, \quad I^{(2)} \sim \frac{\rho_0 U \epsilon}{2\pi R_0} (1 - \tau_1^2)^{-1/2} \left\{ -\frac{KM_2}{\pi a} (1 - 2\tau_1^2) \right\}, \quad (5.30)$$

for  $\tau_1^2 < 1$ , with  $I = 0$  for other values of  $\tau_1$ . The singularity in  $I$ , at  $\tau_1 = \pm 1$ , is a consequence of the abrupt change in thickness of our aerofoil function  $h(x_1)$  at  $x_1 = 0$ . The corresponding results for a smoother profile  $h(x_1)$  are given by formulae (4.54), (4.55), (4.56) and (6.1) and the latter integral will smooth out the square-root singularity.

The integral  $J$  (equation (5.19)) can conveniently be expressed in terms of the dimensionless variables  $\eta$  and  $\tau_1$  of formulae (5.25). Thus

$$J = \frac{\rho_0 UK \epsilon}{2\pi^2 a} \int \frac{\eta(\tau_1 + M_2\eta)}{R \{\eta^2 + (\tau_1 + M_2\eta)^2\}^2} d\eta, \quad (5.31)$$

integrated over all  $\eta$  such that  $(\tau_1 + M_2\eta)^2 + \eta^2 > 1$ , with  $R^2 = X^2 + Z^2 + (Y - a\eta)^2$ . With  $\alpha_1, \alpha_2, \alpha_3$  defined as

$$\alpha_1 = \tau_1 M_2 / (1 + M_2^2), \quad \alpha_2 = \tau_1 / (1 + M_2^2), \quad \alpha_3 = \tau_1 / M_2, \quad (5.32)$$

and the change of variable

$$v = \eta + \alpha_1, \quad (5.33)$$

the integral (5.31) can be expressed as

$$J \sim \frac{\rho_0 U^2 K \epsilon n}{2\pi^2 a} \int_{v_0}^{\infty} \left\{ \frac{F_-}{R_-} + \frac{F_+}{R_+} \right\} dv, \quad (5.34)$$

where

$$F_{\pm}(v) = \frac{(v^2 - \alpha_2^2) \pm v(2\alpha_1 - \alpha_3)}{(v^2 + \alpha_2^2)^2}, \quad (5.35)$$

$$n = Y/R_0, \quad R_{\pm}(v)^2 = X^2 + Z^2 + (Y + \alpha\alpha_1 \pm av)^2, \quad (5.36)$$

and the lower limit  $v_0$ , with  $v_0 \geq 0$ , is given by

$$v_0^2 = \max[0, (1 + M_2^2 - \tau_1^2)/(1 + M_2^2)^2]. \quad (5.37)$$

The approximations  $\beta \sim 1$  and  $1 + M_2^2 \sim 1$  have been used in the analysis leading to formula (5.34); the approximation  $1 + M_2^2 \sim 1$  may also be used in expression (5.37) for the lower limit  $v_0$ . The integral (5.34) is suitable for numerical evaluation, and the pressure contribution  $p_{dis}$  attributed to the displacement sources is then given by formulae (5.16), (5.17), (5.29) and (5.34).

## 5.2. Vortex sound

It remains to calculate the contribution  $\phi_{vor}$  to the potential, arising from the distortion of the vortex tube.

According to Powell (1995) and Howe (1975), there is a connection between moving vortices and the sound field due to distributions of dipoles directed along the common perpendicular to the mean flow and the vorticity. A related representation due to Leppington (1995) for the sound field induced by a moving vortex filament is that of an equivalent dipole sheet, of strength proportional to the circulation constant  $K$ , spread over the surface generated by the path of the vortex line from its distant 'initial' position to its current location specified by  $x = \bar{x}(t, z)$ ,  $y = \bar{y}(t, z)$ . Now the distortions  $\bar{x}$  and  $\bar{y}$  are small (proportional to the aerofoil thickness parameter  $\epsilon$ ) so it is natural to characterize the unsteady sound field in terms of a distribution of dipoles along the  $z$ -axis.

A key identity is the well-known result that a loop vortex line  $C$ , with circulation  $K$ , in incompressible fluid, produces the same velocity field as that due to a distribution of dipoles, of strength  $K$  per unit area, spread over a surface  $S_c$  spanned by  $C$  (for example, see Lamb (1945) §150). In the present context, let  $\delta C$  denote the perimeter of the elementary rectangle  $\delta S_c$  with corners at  $(x, y, z) = (0, 0, z)$ ,  $(0, 0, z + \delta z)$ ,  $(\bar{x}, \bar{y}, z)$  and  $(\bar{x}, \bar{y}, z + \delta z)$ . The additional potential  $\delta\phi_{vor}$ , due to the displaced position  $\bar{x}$ ,  $\bar{y}$  of our vortex line, is therefore equivalent to that of a dipole distribution of strength  $K$ , spread over the elementary area  $\delta S_c$ . With  $\bar{x}$ ,  $\bar{y}$  small, this is equivalent to a point dipole at  $(0, 0, z)$ , of moment  $\delta\mu$ , with

$$\delta\mu = K(\bar{y}, -\bar{x})\delta z. \quad (5.38)$$

The identity described above is for incompressible flow. An estimate for the sound field is obtained by taking the same dipole distribution (5.38), along the  $z$ -axis, and subject to the wave equation with sound speed  $c$ . This amounts to the idea of matching a locally incompressible field with an outer sound field. Thus the outer

potential is given by

$$\phi_{vor} \sim \frac{K}{4\pi} \left\{ \frac{\partial}{\partial x} \int_{-\infty}^{\infty} \frac{\bar{y}(z', t - R/c)}{R} dz' - \frac{\partial}{\partial y} \int_{-\infty}^{\infty} \frac{\bar{x}(z', t - R/c)}{R} dz' \right\}, \quad (5.39)$$

where

$$R^2 = x^2 + y^2 + (z - z')^2, \quad (5.40)$$

and with  $\bar{x}(z, t), \bar{y}(z, t)$  given in terms of the dimensionless variables  $\zeta = z/a$  and  $\tau = Ut/a$  by formulae (4.27) and (4.46).

In the far field, as  $x^2 + y^2 + z^2 \rightarrow \infty$  the most significant terms, from the derivatives in (5.39), are those that correspond to variations of  $\bar{x}$  and  $\bar{y}$  with respect to their second (retarded time) variable. Thus one finds the far-field expressions

$$\phi_{vor} \sim \frac{K}{4\pi} \frac{U}{c} \left\{ -x \int_{-\infty}^{\infty} \frac{\bar{y}_\tau(z', t - R/c)}{R^2} d\zeta' + y \int_{-\infty}^{\infty} \frac{\bar{x}_\tau(z', t - R/c)}{R^2} d\zeta' \right\}, \quad (5.41)$$

where  $\zeta' = z'/a$  and  $\bar{x}_\tau, \bar{y}_\tau$  denote derivatives of  $\bar{x}$  and  $\bar{y}$  with respect to  $\tau$ .

It is convenient to introduce the functions  $I_x(x, y, z; \tau)$  and  $I_y(x, y, z; \tau)$ , defined by the integrals

$$I_x = \int_{-\infty}^{\infty} R^{-2} \{ P_x(\zeta', \tau - (UR/ca)) - P_x(\zeta', \tau - (UR)/(ca) - L/a) \} d\zeta', \quad (5.42)$$

$$I_y = \int_{-\infty}^{\infty} R^{-2} \{ P_y(\zeta', \tau - (UR/ca)) - P_y(\zeta', \tau - (UR)/(ca) - L/a) \} d\zeta', \quad (5.43)$$

where  $P_x(\zeta, \tau)$  and  $P_y(\zeta, \tau)$  are given by equations (4.28), (4.29) and (4.47)–(4.49). The result (5.41) can then be written in the form

$$\phi_{vor} \sim \frac{\epsilon K U}{8\pi^2 c} \left\{ - \left( \frac{K}{\pi a U} \right) x \frac{dI_y}{d\tau} + y \frac{dI_x}{d\tau} \right\}. \quad (5.44)$$

The corresponding pressure fluctuation  $p_{vor}(x, y, z, t)$ , given by

$$p_{vor} = -\rho_0 \frac{\partial \phi_{vor}}{\partial t}, \quad (5.45)$$

with  $\partial/\partial t = (U/a)\partial/\partial\tau$ , therefore has the far-field form

$$p_{vor} \sim p_{vor}^{(x)} + p_{vor}^{(y)}, \quad (5.46)$$

where the  $x$ -dipole and  $y$ -dipole fields  $p_{vor}^{(x)}$  and  $p_{vor}^{(y)}$  are given by

$$p_{vor}^{(x)} \sim \frac{\rho_0 \epsilon K^2 U}{8\pi^3 a^2 c} x \frac{d^2 I_y}{d\tau^2}, \quad p_{vor}^{(y)} \sim -\frac{\rho_0 \epsilon K U^2}{8\pi^2 a c} y \frac{d^2 I_x}{d\tau^2}. \quad (5.47)$$

### 5.3. Distant sound field

The far-field pressure fluctuation  $p$  is the sum of the ‘displacement’ and ‘vortex’ sound contributions described above, thus

$$p = p_{dis} + p_{vor}, \quad (5.48)$$

and the sound pressure level SPL is defined as

$$\text{SPL} = 20 \log_{10} \left\{ \frac{|p|}{2 \times 10^{-5}} \right\}. \quad (5.49)$$

The corresponding expressions

$$\text{SPL}_{dis} = 20 \log_{10} \left\{ \frac{|p_{dis}|}{2 \times 10^{-5}} \right\}, \quad \text{SPL}_{vor} = 20 \log_{10} \left\{ \frac{|p_{vor}|}{2 \times 10^{-5}} \right\} \quad (5.50)$$

are used to compare logarithmic measures of the separate displacement and vortex contributions.

Figure 3(a) shows a graph of SPL, for the point  $(x, y, z) = (100, 100, 50)$  and with the following values for the various parameters:  $U = 150$ ,  $c = 340$ ,  $a = 0.05$ ,  $L = 0.3$ ,  $\epsilon = 0.05$ ,  $K = 15$ ,  $\rho_0 = 1.2$ . The vortex has the most significant distortions when it passes the leading and trailing edges of the aerofoil; our time scale is such that the leading edge passes the centre of the vortex at time  $t = 0$ , and the trailing edge passes the vortex centre at time  $t = L/U$ . The largest distortions of the vortex are near  $z = 0$ , so the most significant contributions to the sound field, arising from the interaction with the leading edge, will reach an observer at  $(x, y, z)$  at times close to  $t_1 = R_1/c$ , where  $R_1^2 = x^2 + y^2 + z^2$ ; similarly, the effect from the interaction with the trailing edge will arrive at times close to  $t_2 = t_1 + L/U$ . In the example of figure 3,  $t_1 = 0.441$  and  $t_2 = 0.443$ , and the acoustic pressure fluctuation is most significant in this vicinity.

Note that the peak values of sound pressure occur in or near the very small time intervals  $t_1 \pm \Delta t$  and  $t_2 \pm \Delta t$ , where  $2\Delta t = 2a/U$  is the time taken for the vortex core to pass the leading edge or trailing edge. The induced pressure decreases rapidly away from those time intervals. The graph is plotted with respect to the scaled time  $\tau_s = (U/a)(t - t_1)$ , with  $t_1 = R_1/c$ . In the small Mach number limit,  $M \rightarrow 0$ , the scaled time  $\tau_s = -1$  corresponds to the arrival of the signal that was launched when the aerofoil first met the surface of the vortex, at the point  $(x, y, z) = (a, 0, 0)$ ; with  $M$  small but non-zero, the corresponding value for  $\tau_s$  is  $\tau_s = -1 - Mx/R_1$  ( $\approx -1.3$  in the example of figure 3). Similarly, the arrival of the signal launched when the aerofoil leading edge meets the back of the vortex (at  $(-a, 0, 0)$ ) is given by  $\tau_s = 1 + Mx/R_1$ ; there are similar contributions arising from the interaction of the vortex with the trailing edges of the aerofoil. Thus peak values for SPL occur near the intervals  $|\tau_s| < 1$  and  $|\tau_s - 6| < 1$  with the value  $L/a = 6$  taken here. The unit of scaled time  $\tau_s = 1$  corresponds to a real time interval  $t = 1/3000$  in this example.

Figure 3(b) shows separately the displacement and vortex sound terms,  $\text{SPL}_{dis}$  and  $\text{SPL}_{vor}$ . It is seen that the displacement sound is dominant at times close to those that correspond to the vortex tube crossing the leading edge and trailing edge. The vortex sound is more significant at other times and should not be ignored.

The extreme peaks in SPL and  $\text{SPL}_{dis}$  at  $\tau_s \approx 1.3$  and at  $\tau_s - 6 \approx 1.3$  correspond to the square-root singularity in formula (5.40) and are a consequence of our choice of a ‘top-hat’ profile for the aerofoil shape function  $h(x_1)$ . This singularity will be smoothed out for a more realistic profile, according to formulae (4.54)–(4.56) and (6.1). The extreme troughs in SPL, near  $\tau_s \approx -1.3, 0.1, 1.3, 4.7, 6.1, 7.3$ , correspond to changes of sign in the pressure fluctuation.

#### 5.4. Total $y$ -dipole strength

It is instructive to consider the total dipole moments that correspond to the ‘displacement’ and ‘vortex’ sound contributions. According to formulae (5.5) and (5.6), the potential  $\phi_{dis}$  is that of a source distribution along the parallel (and moving) lines at  $(x, z) = (-Ut, 0)$  and  $(x, z) = (-Ut + L, 0)$ . The total dipole moment with respect to  $y$  is given by

$$D_{dis}(\tau) = -(\epsilon K a / \pi) \{ \mu_1(\tau) - \mu_1(\tau - L/a) \}, \quad (5.51)$$

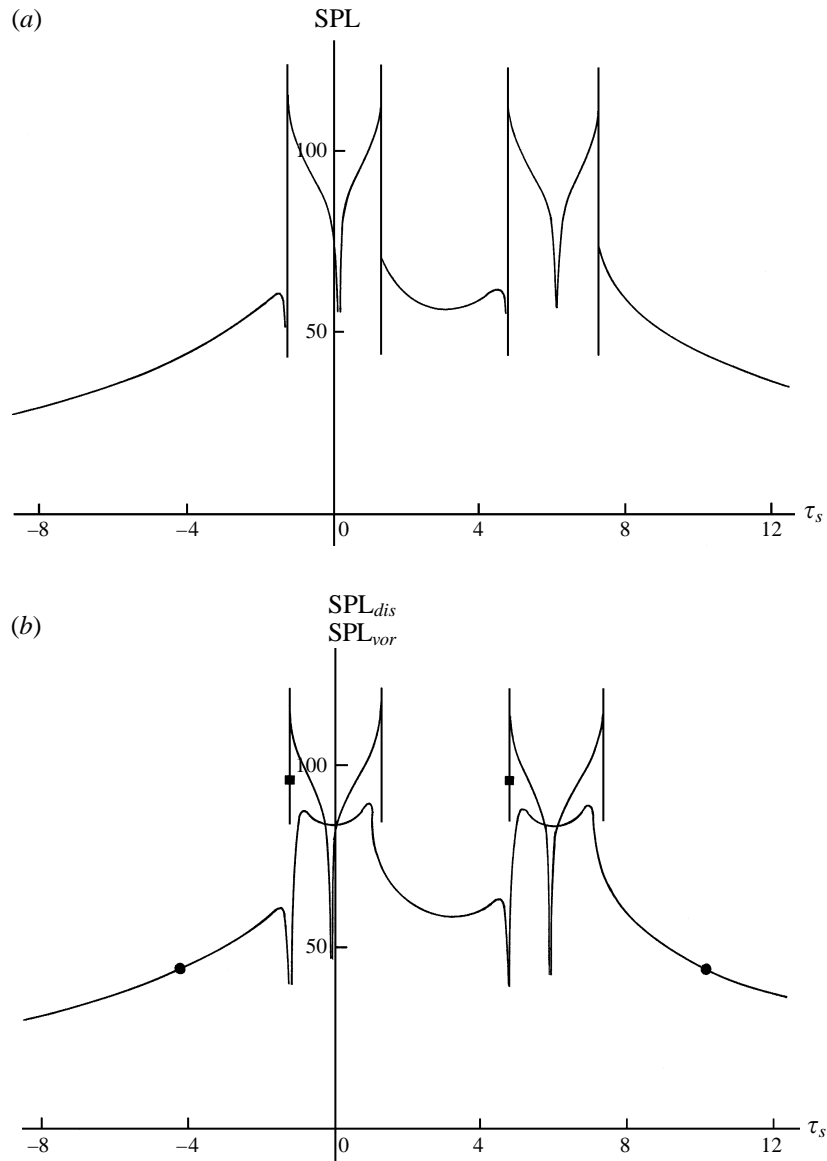


FIGURE 3. Sound pressure level against scaled time  $\tau_s$  at  $(x, y, z) = (100, 100, 50)$ . (a) Graph of SPL; (b) graphs of  $SPL_{dis}$  (—■—) and  $SPL_{vor}$  (—●—).

where  $\tau$  is the dimensionless time variable  $\tau = Ut/a$  and

$$\mu_1(\tau) = \lim_{N \rightarrow \infty} \frac{1}{a} \int_{-N}^N \frac{y^2 H(U^2 t^2 + y^2 - a^2)}{U^2 t^2 + y^2} dy - \frac{2N}{a}. \quad (5.52)$$

The constant  $2N/a$  has been subtracted for convenience, to expedite the limit  $N \rightarrow \infty$ , and does not affect the difference between the two terms in expression (5.51). The integration is elementary and leads to the expression

$$\mu_1 = \begin{cases} -\pi|\tau| & \text{if } |\tau| > 1 \\ -2\tau \sin^{-1} \tau - 2(1 - \tau^2)^{1/2} & \text{if } |\tau| < 1. \end{cases} \quad (5.53)$$

Formulae (5.38) and (5.39) indicate that the ‘vortex’ sound is that due to a distribution of dipoles along the  $z$ -axis. In particular, the total  $y$ -component of the dipole strength is given by

$$D_{vor}(\tau) = -(\epsilon Ka/\pi) \{\mu_2(\tau) - \mu_2(\tau - L/a)\}, \quad (5.54)$$

where, from (4.27),

$$\mu_2(\tau) = \lim_{M \rightarrow \infty} \int_0^M \{P_x(\zeta, \tau) - \ln(\zeta^2)\} d\zeta, \quad (5.55)$$

with  $P_x$  given by (4.28), (4.31), and where the logarithmic term has been subtracted to expedite the limit  $M \rightarrow \infty$ . After some elementary manipulation one finds that

$$\mu_2(\tau) \equiv -\mu_1(\tau), \quad (5.56)$$

given by (5.53). That is, the  $y$ -component of the dipole moment has zero total: the ‘displacement’ and ‘vortex’ contributions are equal and opposite. This does not imply that these  $y$ -dipoles give an insignificant contribution, as they are not concentrated at the origin but are distributed along straight lines, parallel to the  $y$ -axis for the ‘displacement’ terms and parallel to the  $z$ -axis for the ‘vortex’ terms. The identity (5.56) is not unexpected, as it is consistent with the argument used by Howe (1989) and with the general work of Curle (1955) and Ffowcs Williams & Hawkings (1969) who relate the dipole moments to the forces on surfaces: in the present problem the force on the aerofoil has no component in the  $y$ -direction. The identity (5.56) provides a non-trivial test of the algebra in §§4–5.

The above observations are useful in reconciling our results with those due to Howe (1989) in a related problem. The sound field has here been expressed as a sum of five terms, namely

$$p \sim \{I^{(1)}(t) - I^{(1)}(t - L/U)\} + p_{vor}^{(x)} + \{I^{(2)}(t) - I^{(2)}(t - L/U)\} + \{J(t) - J(t - L/U)\} + p_{vor}^{(y)}, \quad (5.57)$$

given by formulae (5.30), (5.34), (5.47) and the functions  $I$  and  $J$  also depend on position as well as time  $t$ . The first term,  $I^{(1)}(t) - I^{(1)}(t - L/U)$ , is the pressure field induced by a source distribution of strength proportional to the derivative  $h'$  of the thickness function, over that part of the aerofoil outside the vortex tube; for the present case, with a rectangular profile, this reduces to a pair of line sources (outside the vortex), at the leading and trailing edges. The last three terms are proportional to  $KU^2n = KU^2y/R$  and correspond to dipoles aligned in the  $y$  direction. Now the total  $y$ -dipole strength is zero, as a consequence of the identity (5.56). The equivalents of these terms are discounted in the problem considered by Howe (1989); in the present context it is argued that they should be retained, as the dipoles are not concentrated at a point but are distributed along infinite straight lines. That leaves the term  $p_{vor}^{(x)}$  which is proportional to  $K^2Ux/R$  and corresponds to a dipole in the  $x$ -direction: this is analogous to the result derived by Howe.

## 6. Concluding remarks

There are several different mechanisms that are relevant to the interaction of a vortex with an aerofoil, and this work concentrates attention on one particular aspect. That is, it aims to estimate the effect when a thin hollow vortex is disturbed as it passes the leading edge of and is displaced from its mean position by a thin symmetric aerofoil. The central idea has been to calculate first the perturbation of the vortex on

the basis of incompressible flow, then to represent the moving vortex tube in terms of an equivalent vortex filament.

Finally, the sound field has been characterized as a sum of ‘displacement’ and ‘vortex’ contributions. These are represented respectively in terms of a distribution of moving monopole sources to account for the displacement effect of the aerofoil, and by a distribution of dipoles of moment related to the distortion of the vortex from its mean position.

As expected, the peak pressures occur as a result of the distortion of the vortex as it passes the aerofoil. One of the dipole terms of expression (5.46) is proportional to the square of the circulation constant  $K$ , in agreement with the prediction of Howe (1989). It is found that the displacement sound is the more significant in the time intervals that correspond to the vortex tube crossing the leading edge and trailing edge. The vortex sound is more significant at other times and should not be ignored.

The analysis does not deal with the effect of the internal structure of the vortex core; the representation of the interior by a hollow, with negligible density and with constant surface pressure, is reasonable for the underwater problem but is less realistic in the aerodynamic case. The corresponding analysis would be much more difficult if a given interior vorticity distribution were imposed. The present model does not account for the larger-scale non-linear distortions of the vortex as it passes the aerofoil, nor for the possibility of axial flow down the core of the vortex. It does not address the separate effect, at a lifting surface, when the vortex tube on the upper and lower surfaces reach the trailing edge at different times, due to the more rapid flow on the upper surface.

The choice of the rectangular aerofoil profile (4.19) is justified on the grounds that the vortex distortion functions  $\bar{x}$  and  $\bar{y}$  can be calculated explicitly in this case, leading to relatively simple expressions (in the form of single integrals) for the displacement and vortex sound contributions. The results are of interest, even though such an aerofoil profile is not physically realistic. Furthermore, any cross-section function  $h(x_1)$  can be generated as a superposition of ‘top-hat’ profiles, according to formula (4.54); the corresponding expressions for  $\bar{x}, \bar{y}$  follow from equations (4.55), (4.56). Similarly, if  $p(x, y, z, t; L)$  is the pressure field given above for the rectangular aerofoil, the solution  $p_h$  for any other two-dimensional aerofoil of cross-section  $h(x_1)$ ,  $0 < x_1 < L$ , is given by

$$p_h = - \int_0^L \frac{dh(l)}{dl} p(x, y, z, t; l) dl. \quad (6.1)$$

This work has been carried out with the support of the Defence Evaluation & Research Agency, Farnborough.

#### REFERENCES

- AMIET, R. K. 1986a Gust response of a flat plate aerofoil in the time domain. *Q. J. Mech. Appl. Maths* **39**, 485–505.
- AMIET, R. K. 1986b Airfoil gust response and the sound produced by airfoil-vortex interaction. *J. Sound Vib.* **107**, 487–506.
- AMIET, R. K. 1990 Gust response of a flat-plate aerofoil and the Kutta condition. *AIAA J.* **28**, 1718–1727.
- CURLE, N. 1955 On the influence of solid bodies upon aerodynamic sound. *Proc. R. Soc. Lond. A* **231**, 505–514.

- FFOWCS WILLIAMS, J. E. & GUO, Y. P. 1988 Sound generated from the interruption of a steady flow by a supersonically moving aerofoil. *J. Fluid Mech.* **195**, 113–135.
- FFOWCS WILLIAMS, J. E. & HAWKINGS, D. L. 1969 Sound generation by turbulence and surfaces in arbitrary motion. *Phil. Trans. R. Soc. Lond. A* **264**, 321–342.
- FFOWCS WILLIAMS, J. E. & O'SHEA, S. 1970 Sound generation by hydrodynamic sources near a cavitated line vortex. *J. Fluid Mech.* **43**, 675–688.
- HAWKINGS, D. L. 1978 A possible unsteady thickness noise mechanism for helicopter rotors. *95th Meeting of the Acoustical Society of America, Providence, RI*.
- HOWE, M. S. 1975 Contributions to the theory of aerodynamic sound, with application to excess jet noise and the theory of the flute. *J. Fluid Mech.* **71**, 625–673.
- HOWE, M. S. 1989 On unsteady surface forces, and sound produced by the normal chopping of a rectilinear vortex. *J. Fluid Mech.* **206**, 131–153.
- HOWE, M. S. 1991 On the estimation of sound produced by complex fluid-structure interactions, with application to a vortex interacting with a shrouded rotor. *Proc. R. Soc. Lond. A* **433**, 573–598.
- JANAKIRAM, R. D. 1990 Aeroacoustics of rotorcraft. *AGARD Report 781*.
- KAMBE, T. 1986 Acoustic emissions by vortex motions. *J. Fluid Mech.* **173**, 643–666.
- LAMB, H. 1945 *Hydrodynamics*, 6th edn. Dover.
- LEPPINGTON, F. G. 1995 The interaction between sound and circulatory fluid motion as a problem in matched expansions. *IMA J. Appl. Maths* **55**, 163–186.
- LIGHTHILL, M. J. 1952 On sound generated aerodynamically. I. General theory. *Proc. R. Soc. Lond. A* **211**, 564–585.
- MÖHRING, W. 1978 On vortex sound at low Mach number. *J. Fluid. Mech.* **85**, 685–691.
- MOORE, D. W. 1974 A numerical study of the roll up of a finite vortex sheet. *J. Fluid Mech.* **63**, 225–235.
- MOORE, D. W. & SAFFMAN, P. G. 1973 Axial flow in laminar trailing vortices *Proc. R. Soc. Lond. A* **333**, 491–508.
- POWELL, A. 1964 Theory of vortex sound. *J. Acoust. Soc. Am.* **35**, 1133–1143.
- POWELL, A. 1995 Vortex sound: an alternative derivation of Möhring's formulation. *J. Acoust. Soc. Am.* **97**, 684–686.
- SCHMITZ, F. H. & YU, Y. H. 1986 Helicopter impulsive noise: theoretical and experimental status. *Recent Advances in Aeroacoustics* (ed. A. Krothapalli & C. A. Smith), pp. 149–243. Springer.
- SOZOU, C. 1990 Resonant interaction of a sound wave with a cylindrical vortex. *J. Acoust. Soc. Am.* **87**, 2342–2348.
- WATSON, G. N. 1944 *Theory of Bessel functions*. Cambridge University Press.